



STANFORD
CANCER INSTITUTE



Activating cGAS-STING Signaling in Breast Cancer

November 2020

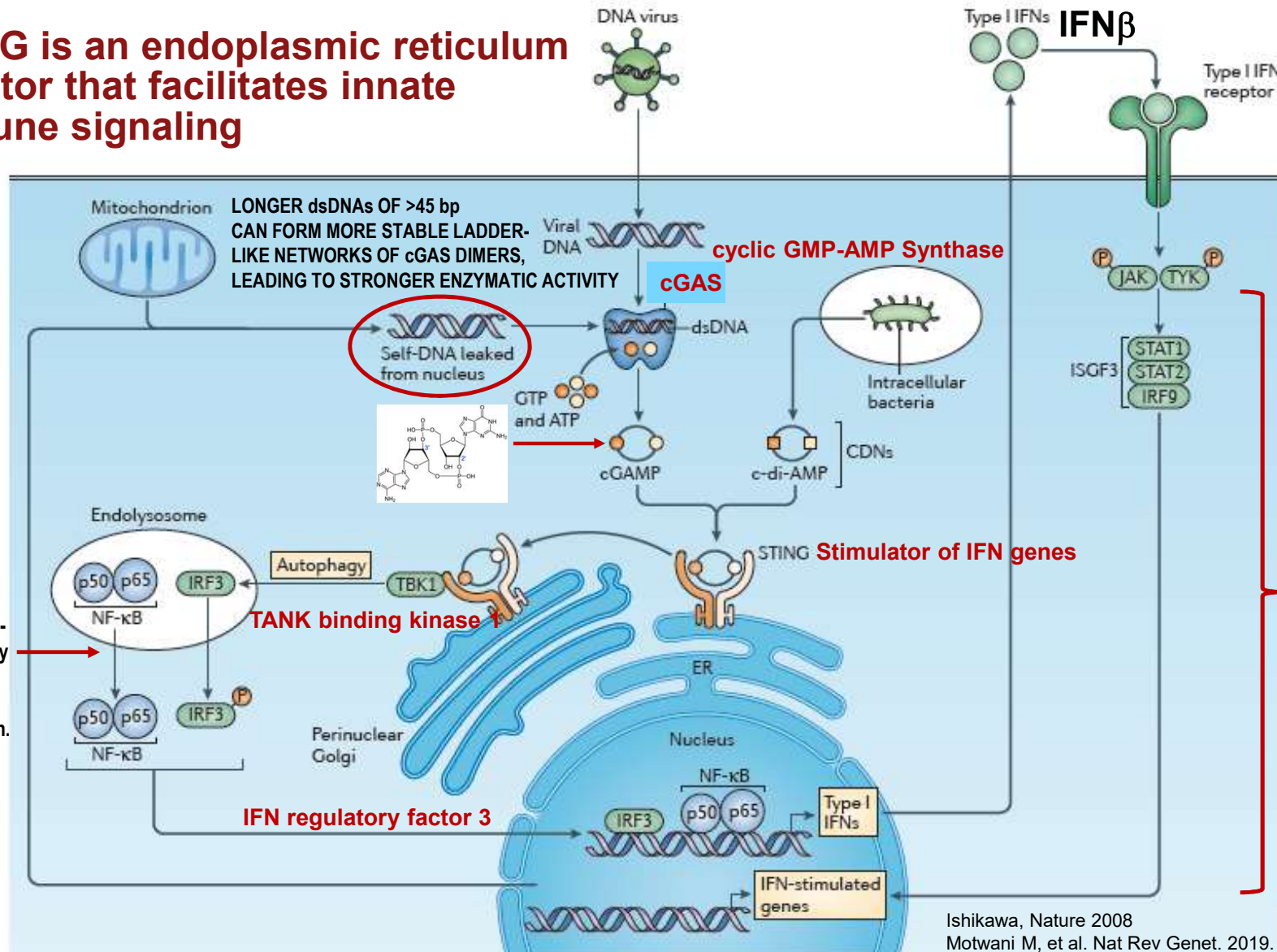


Mark D. Pegram, M.D.
Susy Yuan-Huey Hung Professor of Oncology
Associate Director for Clinical Research
Associate Dean for Clinical Research Quality
Stanford University School of Medicine

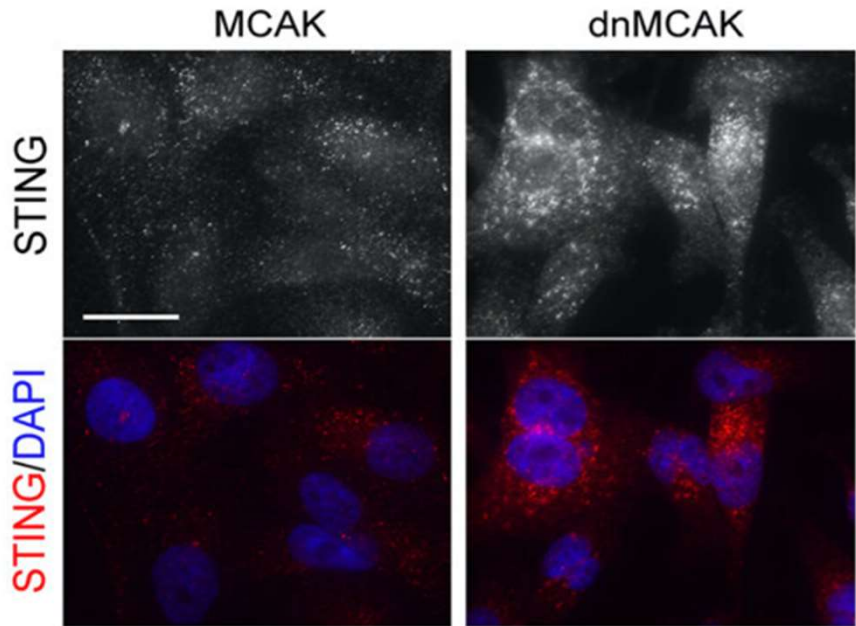
Conflicts relevant to topic – Roche/GNE, Novartis



STING is an endoplasmic reticulum adaptor that facilitates innate immune signaling

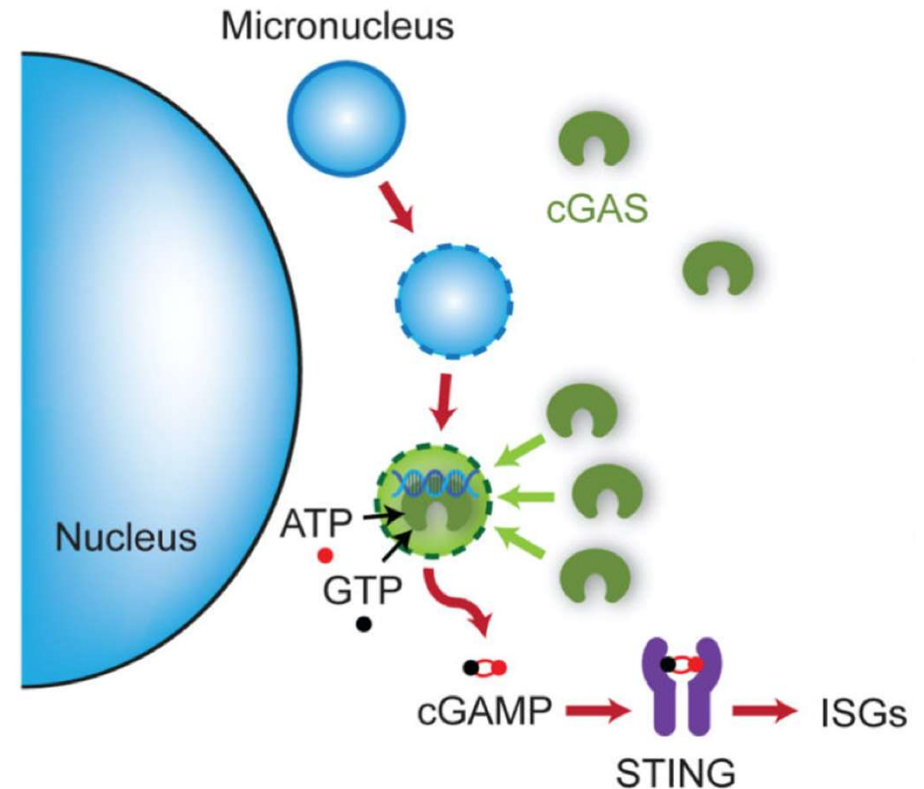


Model: Micronuclear membrane rupture leads to cGAS sensing of DNA



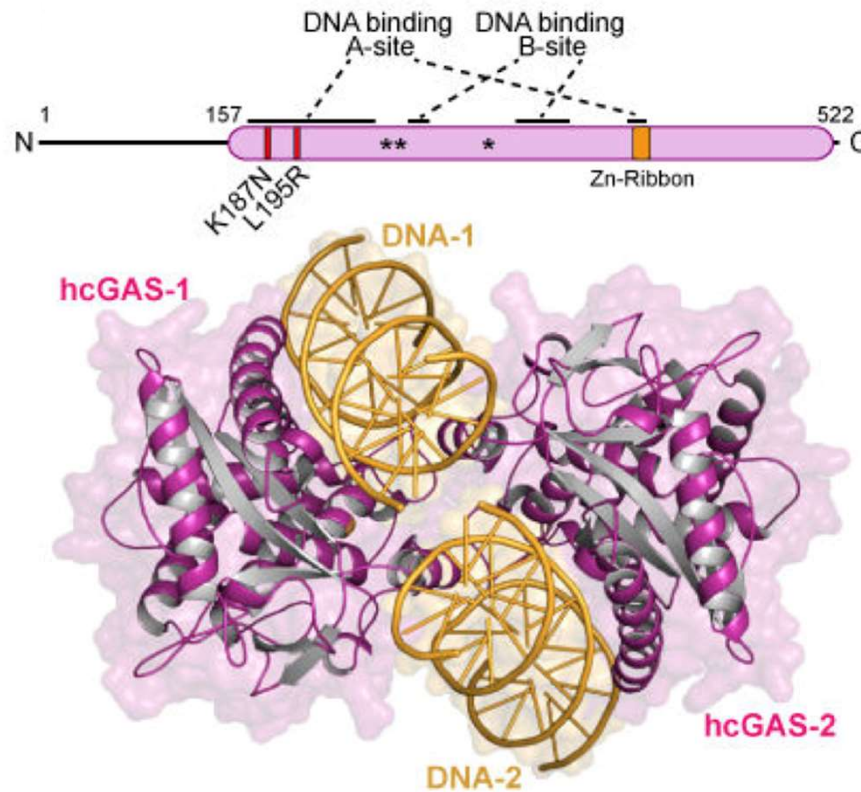
Expression of STING (Stimulator of IFN Genes), red, in MCAK and dnMCAK 231 cells.

Samuel F. Bakhroum, ... Lewis C. Cantley, et al.
 Nature. 2018 January 25; 553(7689): 467-72.



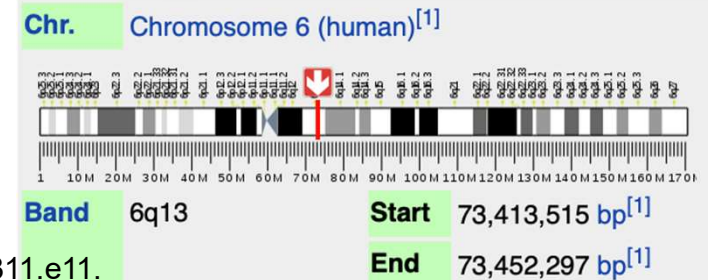
Micronuclei are susceptible to nuclear envelope collapse, which permits cytosolic cGAS access to genomic dsDNA, initiating a cGAS-STING dependent proinflammatory immune response through production of the second messenger cGAMP
 Wang et al. Nature. 2017 August 24; 548(7668): 461-465.

cGAS -- Cyclic GMP-AMP synthase (AKA cGAMP synthase),

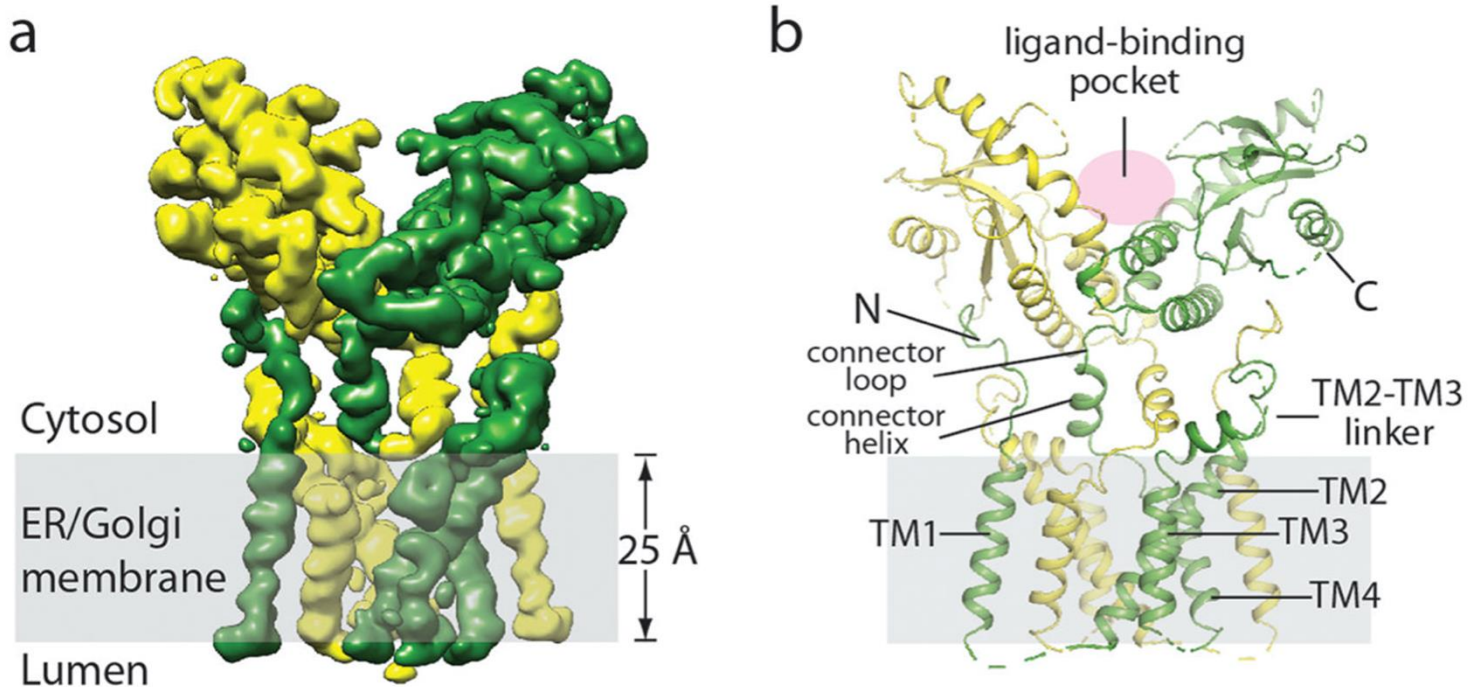


Schematic and overview of the hcGAS–DNA complex. hcGAS forms a 2:2 complex with DNA where each cGAS monomer has two distinct DNA-binding surfaces (DNA A-Site and DNA B-Site). Stars in the schematic denote the enzyme metal-coordinating active-site residues, schematic not to scale. K187N and L195R are regulatory adaptations in human cGAS that balance enzymatic activity with DNA-length sensitivity.

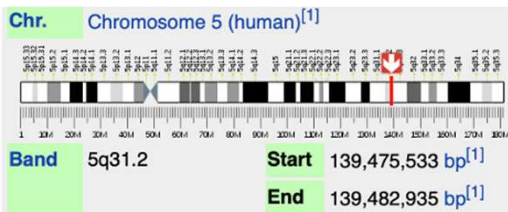
Human cGAS is encoded by the MB21D1 gene



Cryo-EM structures of hSTING reveal its mechanism of activation by cyclic GMP-AMP

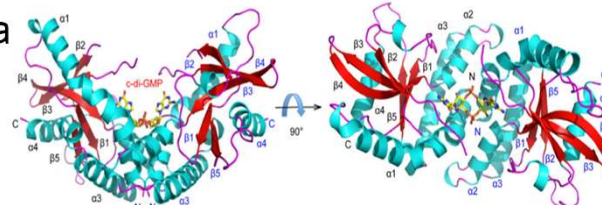


a, Side view of the cryo-EM 3D reconstruction. The two subunits in the dimer are coloured



TMEM173 gene: 5q31.2

reen. b, Ca



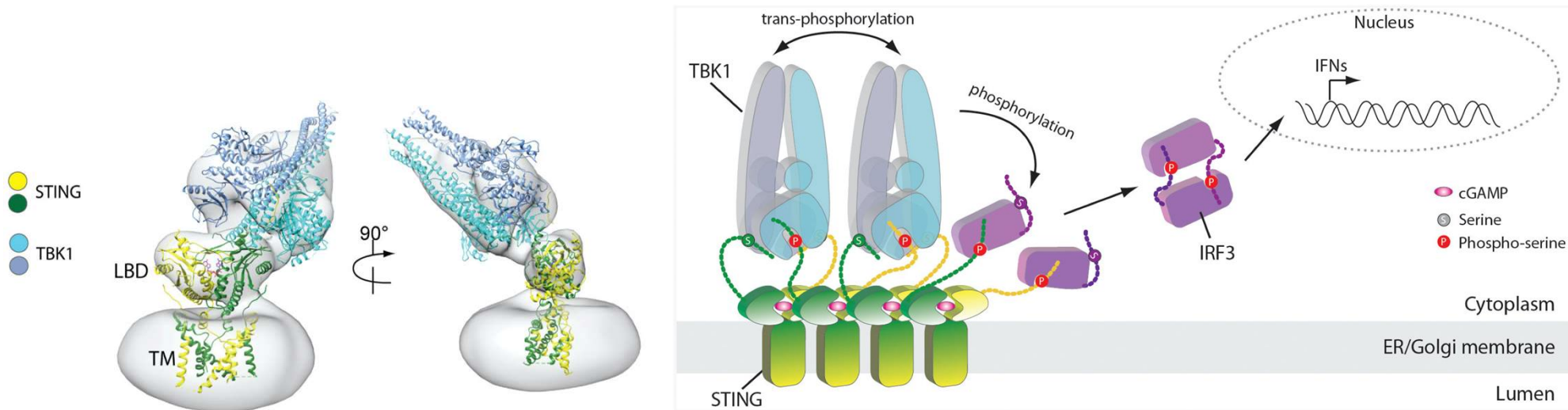
Structure of human STING CTD bound to c-di-GMP. STING is shown by the red and cyan ribbon representation. C-di-GMP is shown by the yellow ball and stick model.

e in two orthogonal side

Chang Shu, et al. Nat Struct Mol Biol. 2012 Jul; 19(7): 722–724.

Guijun Shang, et al. Nature. 2019 March ; 567(7748): 389–

Cryo-electron microscopy structure of human TBK1 in complex with cGAMP-bound, full-length chicken STING



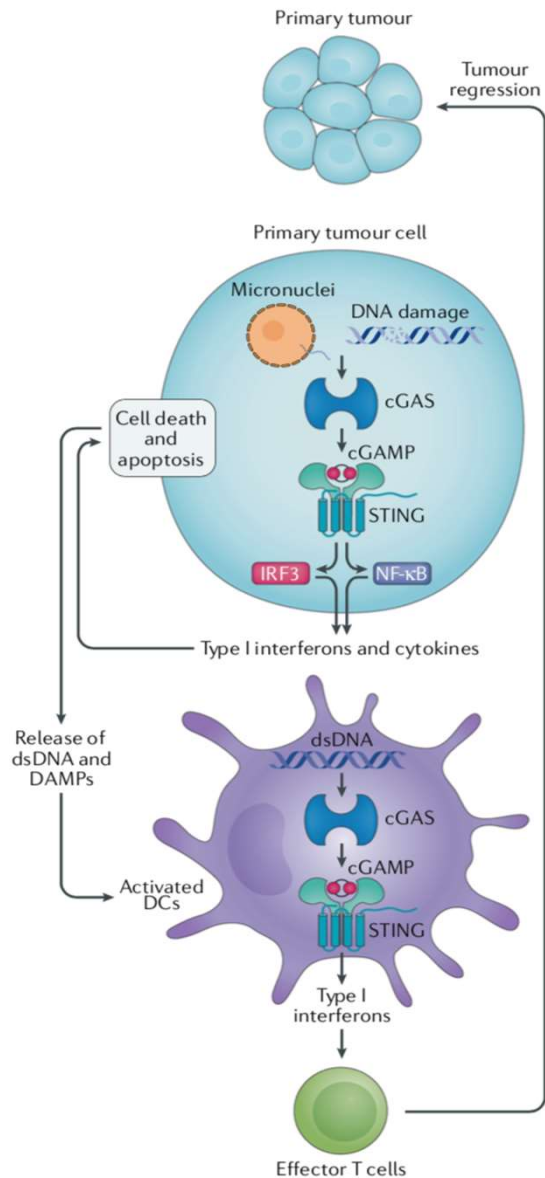
Extended Data Fig. 7 | Cartoon model of STING-mediated activation of TBK1 and the downstream signalling pathway.

The cGAMP-induced oligomerization of STING leads to TBK1 clustering and trans-autophosphorylation. Activated TBK1 phosphorylates STING C-terminal tails that are not bound to the SDD-kinase domain groove in TBK1. Phosphorylated tails of STING recruit IRF3, which is phosphorylated by TBK1. Phosphorylated IRF3 forms a dimer and translocates to the nucleus to initiate the transcription of IFN genes.

Regulation of the cGAS-STING pathway – importance of post-translational events (post-translational modifications and protein-protein interactions):

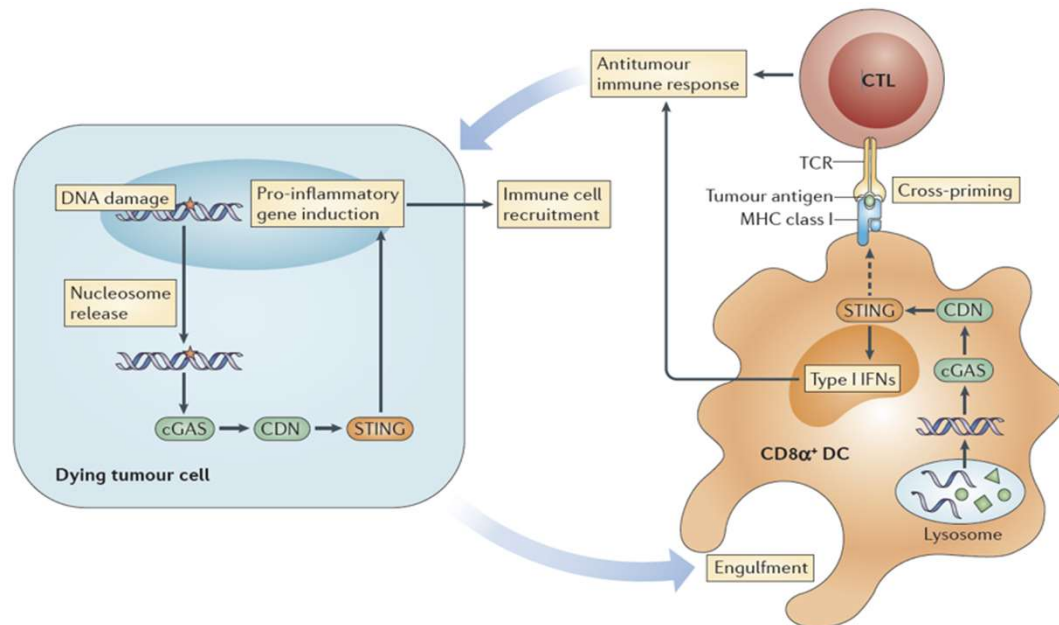
	Modification	Molecules	Mechanism	Residues/domains
cGAS	Deglutamylation	CCP5 and CCP6	Enhanced enzymatic activity	Removal of glutamate chain at E302 and E272
	SUMOylation	TRIM38	Increased stability	NA
	DeSUMOylation	SENP7	Enhanced activation	NA
	Ubiquitination	RINCK (also known as TRIM41)	Increased cGAMP synthesis	NA
		RNF185	Enhanced enzymatic activity	K27-linked polyubiquitination at K173 and K384
		TRIM56	Enhanced cGAMP production	Monoubiquitination at K335
	Deubiquitination	TRIM14	Enhanced stability	Recruits USP18 to cleave K48-linked ubiquitination at K414
		USP14	Enhanced stability	K48-linked ubiquitination at K414
	Protein–protein binding	G3BP1	Increased DNA-binding affinity	Binds to N terminus of cGAS
		PQBP1	Enhanced cGAMP production	Binds to cGAS via PQBP1 WW domain
ZCCHC3		Enhanced oligomerization	Binds to NTase and the C-terminal fragment of cGAS	
STING	Palmitoylation	NR	STING activation	Palmitoylation at C88 and C91 of STING
	Ubiquitination	AMFR	Translocation from the ER via Golgi	K27-linked polyubiquitination
		TRIM32	Enhanced interaction with TBK1	K63-linked ubiquitination at K20, K150, K224 and K236
		TRIM56	Enhanced interaction with TBK1	K63-linked ubiquitination at K150
		RNF26	Prevention of degradation	K11-linked polyubiquitination at K150
		UBXN3B	Facilitates STING–TRIM56 interaction	TRIM56-mediated K63-linked ubiquitination via UAS domain of UBXN3B
		MUL1 (also known as RNF218)	Facilitates STING trafficking	K63-linked polyubiquitination at K224
	Deubiquitination	ZDHC1	Maintenance of stability and STING aggregation	K48-linked polyubiquitination; N terminus of STING interacts with the N terminus of ZDHC1
		CYLD	STING stabilization	K48-linked polyubiquitination via CYLD USP domain
	Protein–protein binding	SAR1A and SEC24C	Facilitates STING trafficking	NA
		DDX41	Enhanced STING signalling	DDX41 binds to transmembrane domains
		IFI16	Enhanced STING activation	IFI16 interacts with STING via PYRIN domain
		IRHOM2	Recruitment of TRAP β for STING trafficking	Interaction via transmembrane domains

Motwani M, et al. Nat Rev Genet. 2019.

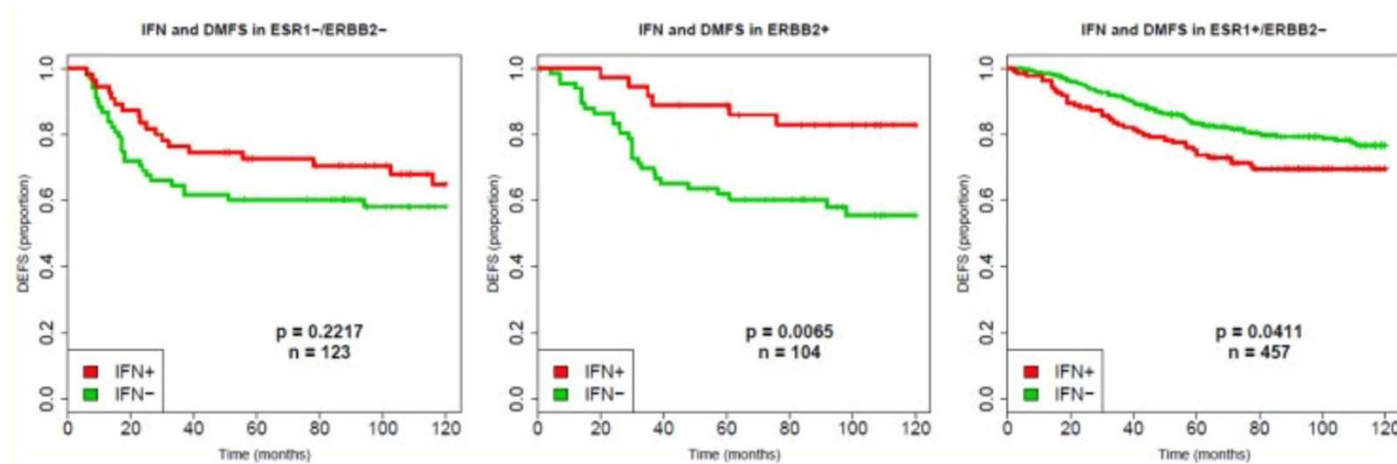


An essential link between innate and adaptive immunity is provided by dendritic cells

Uptake of dsDNA and tumor antigens by tumor-resident dendritic cells (DCs) elicits a complimentary cGAS–STING-dependent type I interferon-mediated activation of an antitumor immune response, for example, through activation of effector T cells such as tumor-associated, antigen-specific CD8⁺ T cells, which can destroy tumor cells.



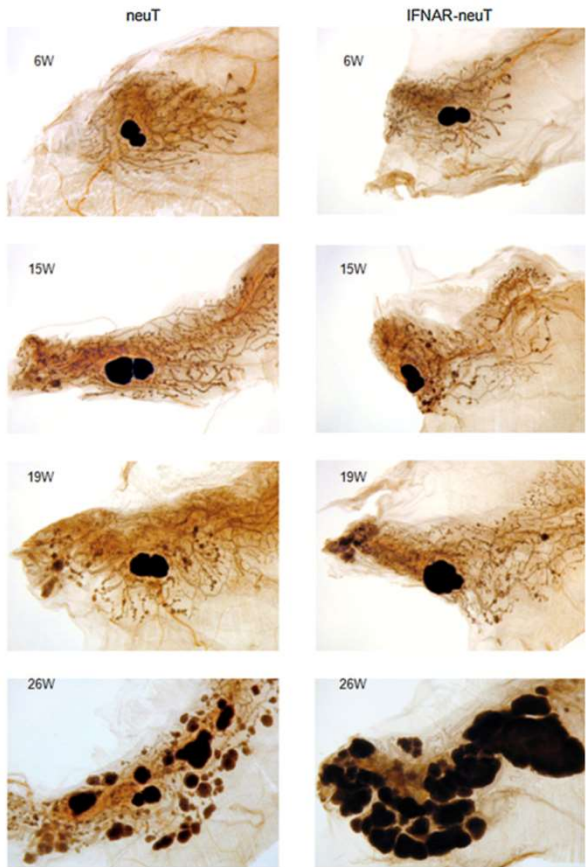
Subtype-dependent prognostic relevance of an interferon-induced pathway metagene in node-negative breast cancer



Kaplan–Meier curves (DMFS) according to the IFN metagene status (33% of patients with tumors with the highest IFN metagene expression were defined as IFN+, the remaining patients were considered IFN-) in ESR1-/ERBB2-, ERBB2+ and ESR1+/ERBB2- tumors.

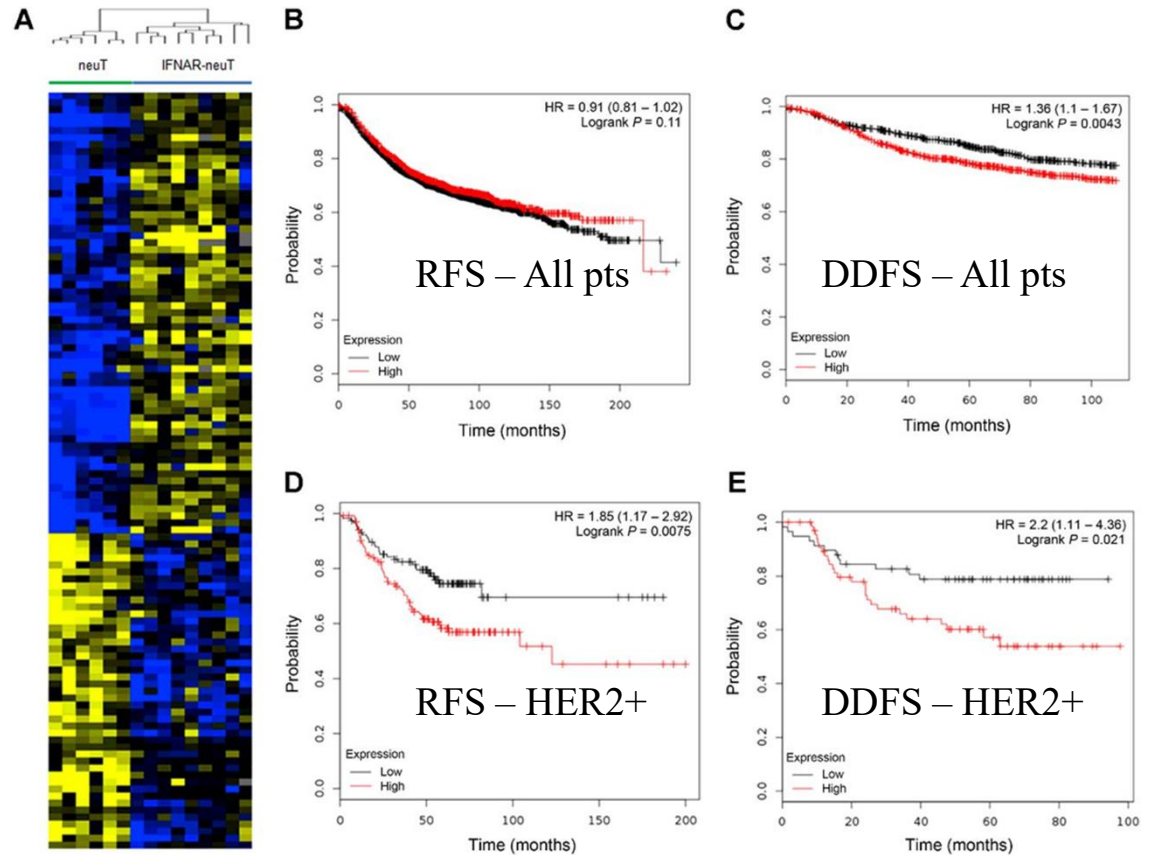
Disruption of IFN-I Signaling Promotes HER2/Neu Tumor Progression

Neu transgenic (neuT) Nonfunctional mutation in the IFN-I receptor (IFNAR1)



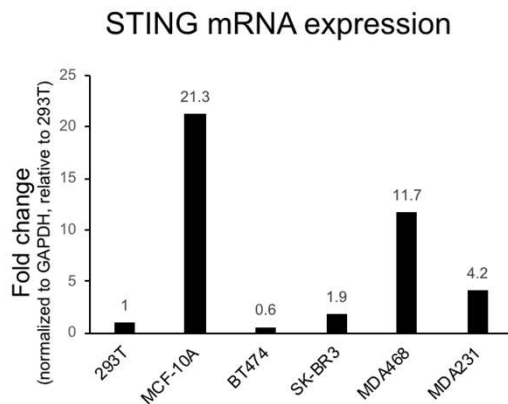
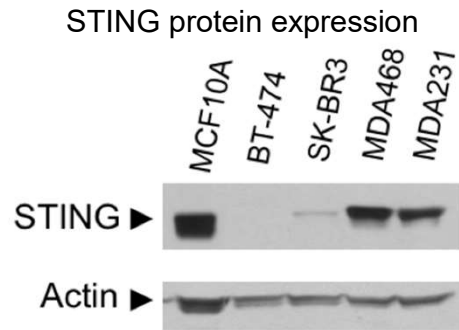
Earlier onset, higher mean tumor multiplicity and accelerated growth of mammary tumors in IFNAR-neuT mice.

IFNAR-neuT tumors show molecular signature shared with certain subtypes human breast cancer patients.

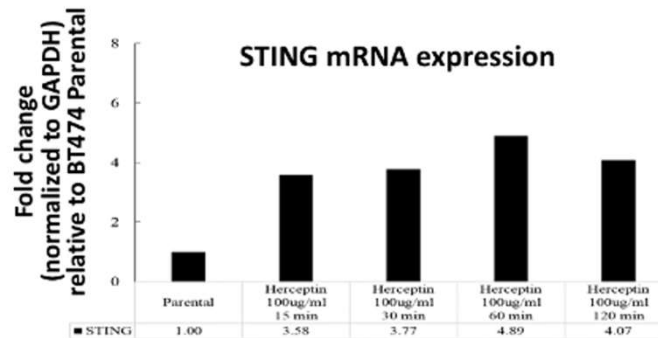


Clustered heatmap of the 118 genes differentially expressed ($P < 0.005$, random-variance T test) between neuT (green bar) and IFNAR-neuT (blue bar) tumor lesions, isolated from 19-week-old transgenic mice.

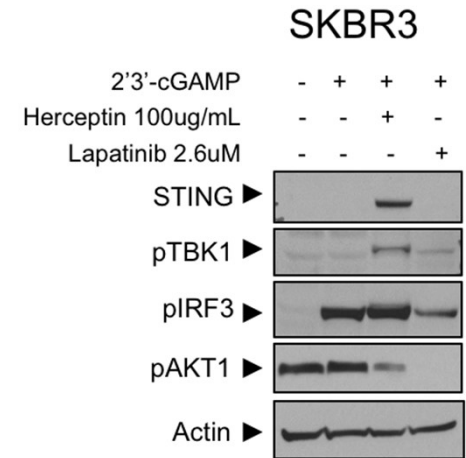
STING expression in HER2+ breast cancer cells +/- trastuzumab



STING protein immunoblot (above) and mRNA expression (below) in HER2+ BT474 and SKBR3 cells, compared to MCF10A mammary epithelial cells and triple negative MDA468 and MDA231 cells.



STING mRNA expression by real time PCR before and following trastuzumab At 15, 30, 60 and 120 mins (p=0.001).



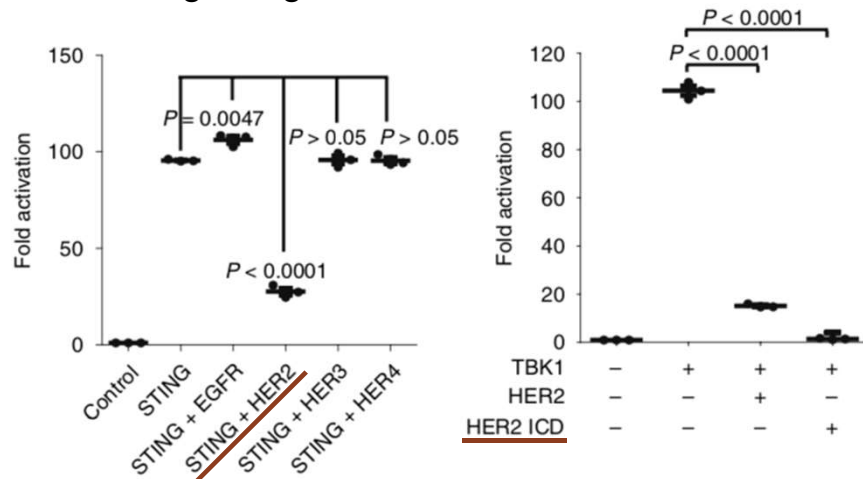
Reconstitution of STING, pTBK1, and pIRF3 in HER2+ SKBR3 cells following 2'3'-cGAMP and trastuzumab.

Stanford University
Amy Zong, Pegram Lab, unpublished data

HER2 recruits AKT1 to disrupt STING signalling and suppress antiviral defence and antitumour immunity

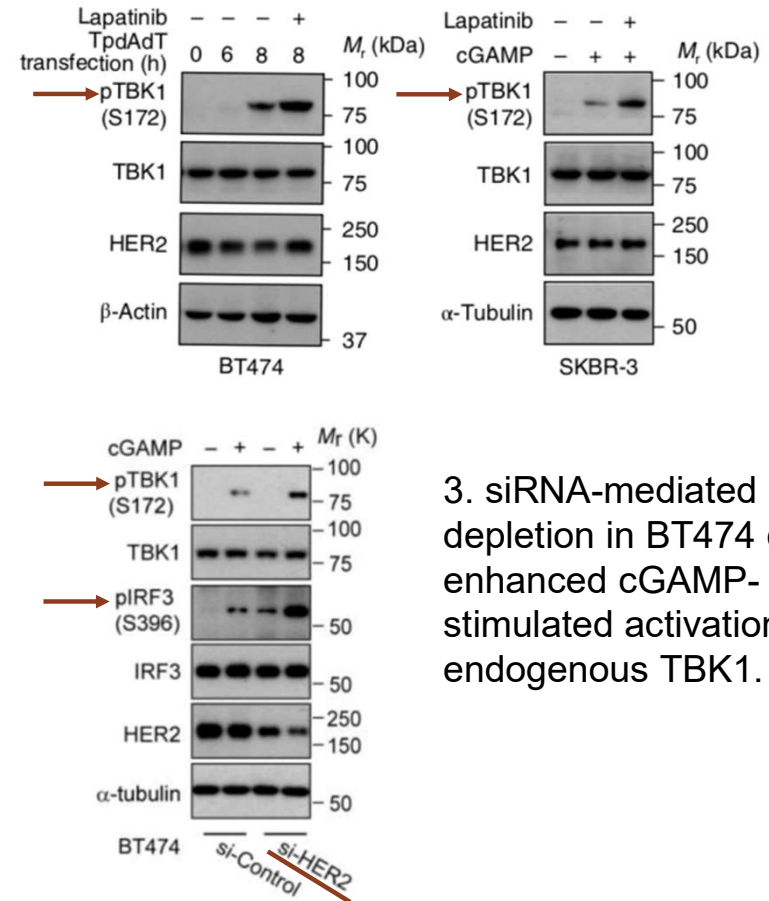
Shiyong Wu^{1,8}, Qian Zhang^{1,2,8}, Fei Zhang^{1,8}, Fansen Meng^{1,2}, Shengduo Liu¹, Ruyuan Zhou¹, Qingzhe Wu¹, Xinran Li¹, Li Shen¹, Jun Huang¹, Jun Qin³, Songying Ouyang⁴, Zongping Xia⁵, Hai Song¹, Xin-Hua Feng^{1,6}, Jian Zou⁷ and Pinglong Xu^{1,2*}

1. Screening of the tyrosine kinome cDNA library revealed HER2 to be a strong suppressor of STING signaling.



Luciferase-reporter assay with an IRF3-responsive ISRE promoter stimulated by STING coexpression in HEK293 cells.

2. Lapatinib potentiated poly(dA:dT) DNA analogue TpdAdT- or cGAMP-induced STING signaling in the HER2-driven tumor lines BT474 (left) and SKBR-3 (right).



3. siRNA-mediated HER2 depletion in BT474 cells enhanced cGAMP-stimulated activation of endogenous TBK1.

Table 1. STING expression in the tumor cell compartment of breast cancer patients by IHC

	ER+/HER2- (N=102)	HER2+ (N=57)	TNBC (N=39)
	<i>no. of patients (%)</i>		
0	53 (52.0%)	38 (66.7%)	28 (71.8%)
1+	25 (24.5%)	10 (17.5%)	5 (5.1%)
2+	16 (15.7%)	9 (15.8%)	2 (5.1%)
3+	8 (7.8%)	0	4 (10.3%)
N total = 198			<i>P=.055</i>

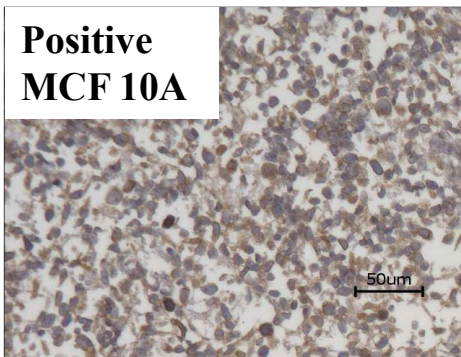
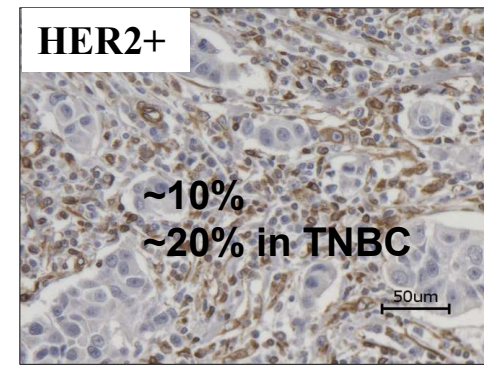
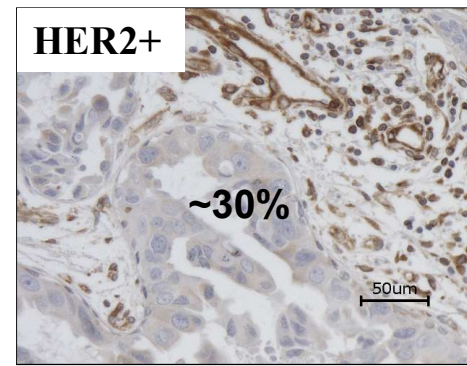
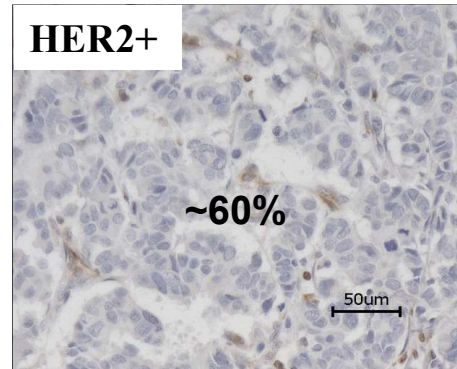
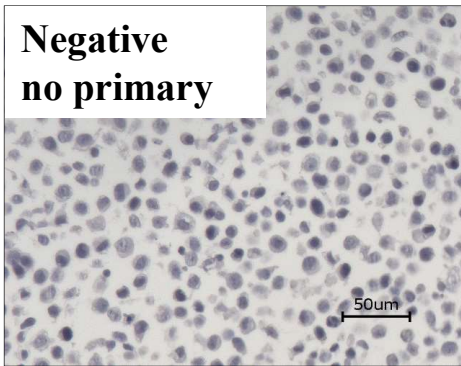
Invasive Breast Cancer Patients: STING expression and pattern

Controls

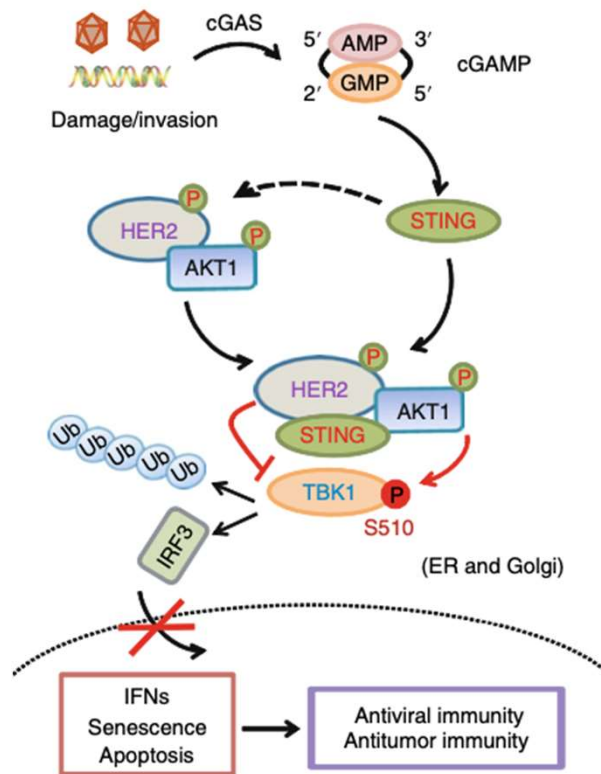
Immune Desert

Margin/Stroma Restricted

Inflamed



HER2 protects cancer cells from STING-mediated antitumour immunity



- Cytosolic sensing of DNA not only leads to cGAMP production and the assembly of the STING signalosome but also activates the HER2–AKT1 axis, which is recruited by STING and modifies TBK1 directly at the S510 residue to impede the assembly of the STING signalosome.
- HER2-mediated suppression of cytosolic DNA sensing is crucial to prevent cells from exacerbating their damage, suppress danger responses to the production of IFNs, senescence or apoptosis and, in the tumour setting, to enhance the tolerance of tumour cells to antitumour immunity.

STING Activation and its Application in Immuno-Oncology

Identifier	Compound	Sponsor	Phase	Disease (Route of Administration)	Regimen	Primary endpoint	Start date
NCT02675439	ADU-S100 (MIW815)	Aduro, Novartis	I	Advanced/metastatic solid tumors or lymphomas (IT)	+/-Ipilimumab (CTLA4)	AEs, RP2D	Mar 2016
NCT03172936	ADU-S100 (MIW815)	Novartis	I	Advanced/metastatic solid tumors or lymphomas (IT)	+ spartalizumab (PD1)	DLTs	Sept 2017
NCT03010176	MK-1454	Merck	I	Advanced/metastatic solid tumors or lymphomas (IT)	+/- Pembrolizumab (PD1)	DLTs, AEs	Feb 2017
NCT04220866	MK-1454	Merck	II	Metastatic or unresectable, recurrent head and neck squamous cell carcinoma (HNSCC) (IT)	MK-1454+ Pembrolizumab vs. Pembrolizumab	ORR	Mar 2020
NCT03843359	GSK3745417	GSK	I	Advanced Solid Tumors (IV)	+/- Pembrolizumab	DLTs, AEs, ORR	Mar 2019
NCT03956680	BMS986301	BMS	I	Advanced Solid Tumors (IT)	BMS986301→ Nivolumab (PD1)+ Ipilimumab (CTLA4)	DLTs, AEs	Mar 2019
NCT04096638	SB11285	Spring Bank Pharmaceuticals	I	Advanced Solid Tumors (IV)	+/- Nivolumab	DLTs, MTD, RP2D, AEs	Sept 2019
NCT04144140	E7766	Eisai	I	Advanced solid tumors or lymphomas (IT)	E7766 alone	DLTs, AEs, ORR, DOR, CBR	Mar 2020
NCT04109092	E7766	Eisai	I	Non-muscle Invasive Bladder Cancer (NMIBC) unresponsive to BCG Therapy (Intravesical)	E7766 alone	DLTs, AEs, CRR at 3mo, 6mo, 12mo, 18mo, 24mo	Feb 2020

Abbr.: IT, intratumoral; IV, intravenous; AEs, adverse events; RP2D, recommended phase 2 dose; DLTs, dose-limiting toxicity; ORR, objective response rate; CRR, complete response rate; MTD, maximum tolerated dose

Stanford University

STING agonist combined with check-point inhibitor

- Phase I Study of MK-1454 Alone or in Combination With Pembrolizumab in Participants With Advanced/Metastatic Solid Tumors or Lymphomas (MK-1454-001)

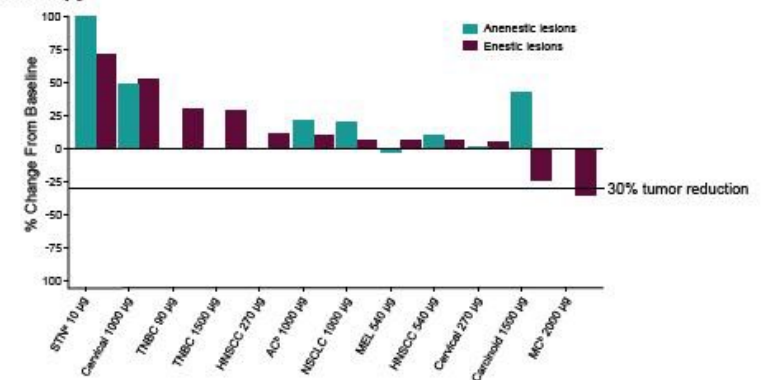
Table 4. Summary of Best Overall Response With Confirmation Based on Investigator Assessment per RECIST 1.1 (FAS Population)

Response n (%)	Arm 1 Monotherapy Total N=20 ^a	Arm 2 Combination Therapy Total N=25 ^{a,b}
Complete response	0 (0.0)	0 (0.0)
Partial response	0 (0.0)	6 (24.0)
Stable disease	4 (20.0)	6 (24.0)
Disease control	4 (20.0)	12 (48.0)
Progressive disease	9 (45.0)	9 (36.0)
Nonevaluable ^c	1 (5.0)	0 (0.0)
No assessment ^d	6 (30.0)	4 (16.0)

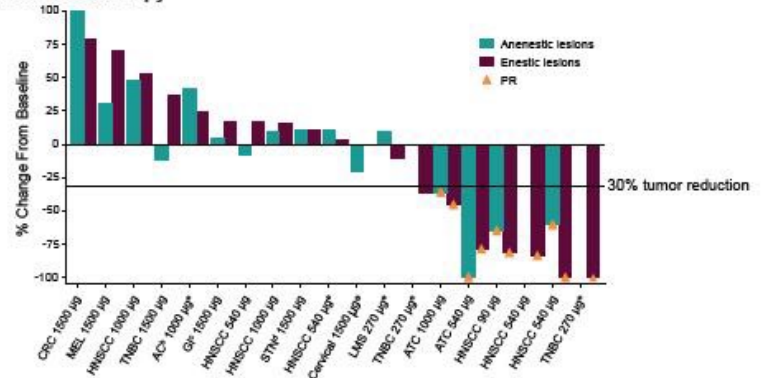
Only response evaluation after crossover is included in the calculation of best overall response in Arm 2. ^aFAS=full analysis set; ^bIncludes 9 patients who crossed over from monotherapy (Arm 1); ^cNonevaluable includes patients with insufficient data for assessment of response per RECIST 1.1; ^dNo assessment includes patients without post-baseline assessment as of data cutoff date. Only patients who were first-dosed by May 1, 2018, are included.

Figure 3. Maximum Percentage Change From Baseline in Target Injected (Enestic) vs Non-injected (Anesthetic) Lesions (Investigator Review, RECIST 1.1)

A. Monotherapy



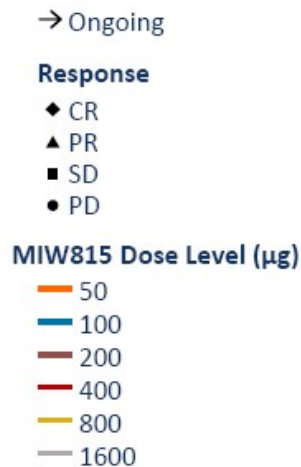
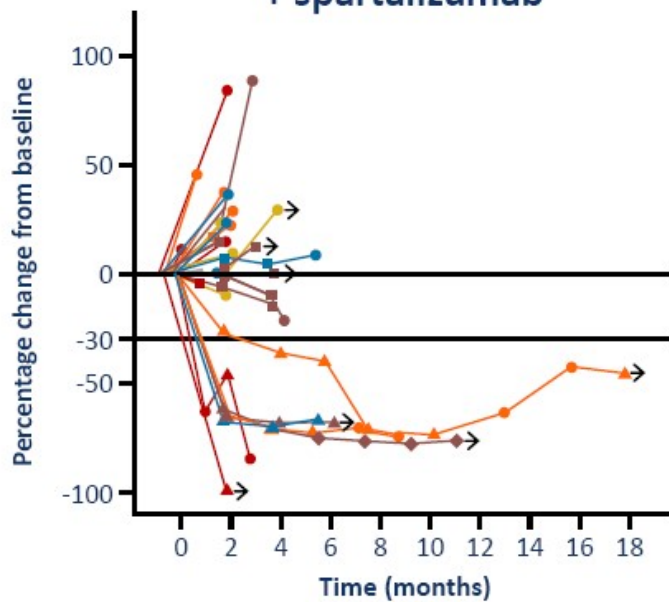
B. Combination Therapy



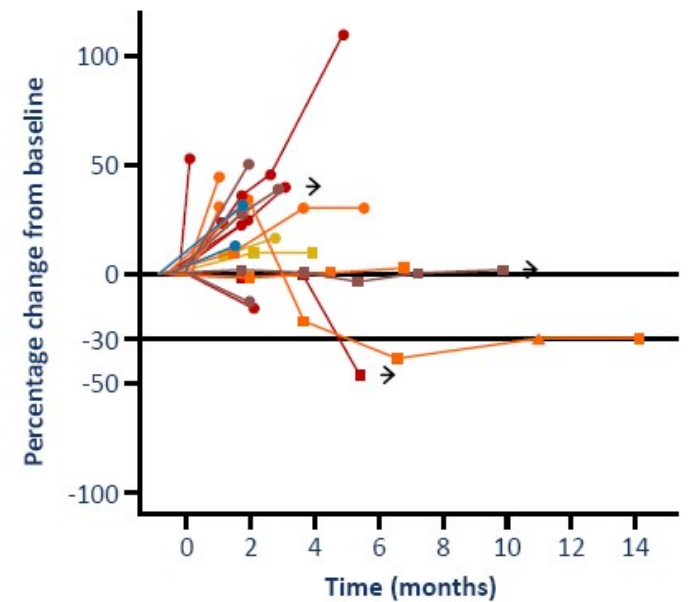
STING agonist combined with check-point inhibitor

- Phase Ib study of MIW815 (ADU-S100) in combination with spartalizumab (PDR001) in patients with advanced/metastatic solid tumors or lymphomas (NCT03172936)

MIW815 weekly (3-weeks-on/1-week-off)
+ spartalizumab



MIW815 monthly + spartalizumab



AT-rich STING activating 90bp dsDNA ligand (STING-dependent adjuvants, STAVs) activate cGAS-STING-TBK1-IRF3 signaling; phagocytosis of STAV-transduced, UV-irradiated tumor cells by macrophages stimulates cytokine

expression in trans

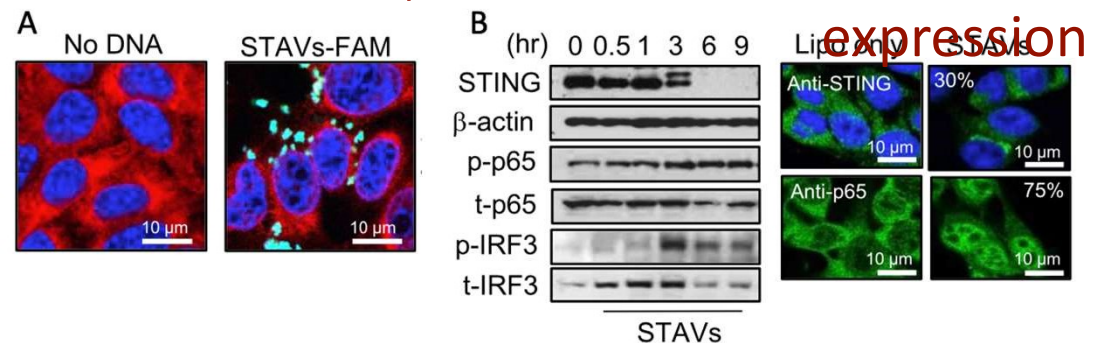


Figure 2. (A) Confocal analysis of B16 OVA cells (B16) transfected with FAM-labeled STAVs (green). DAPI (blue), and anti-calreticulin (red) as counter staining. (B, left) Western blot analysis of STING, p65 NF-κB, and IRF3 in B16 cells transfected with 3 mg/mL STAVs and incubated for time courses indicated. (B, right) Immunofluorescent microscopy analysis using anti-STING and anti-p65 in B16 cells at 3 hr after STAV transfection (3 mg/mL) demonstrates STING re-localization from the cytoplasm to peri-nuclear Golgi, and nuclear localization of p65 NF-κB following STAV transduction.

Jeonghyun Ahn,...Glen N. Barber. Extrinsic Phagocyte-Dependent STING Signaling Dictates the Immunogenicity of Dying Cells. 2018, Cancer Cell 33, 1–12

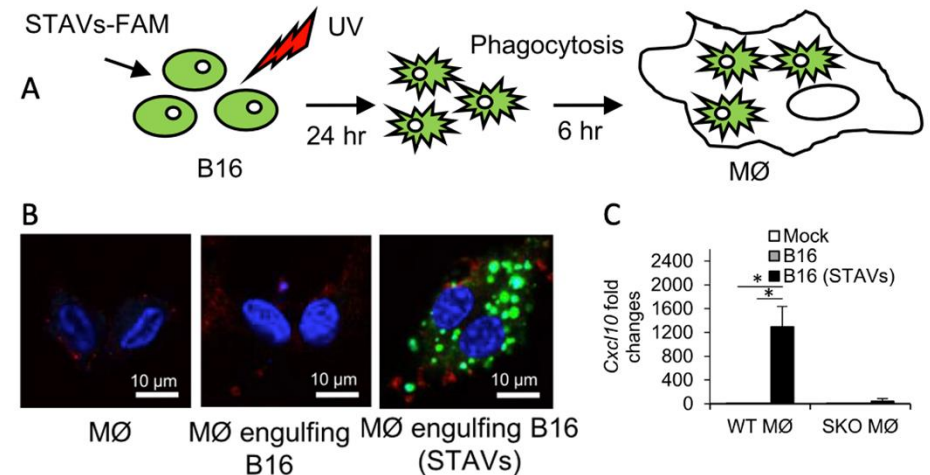


Figure 3. (A) Schematic representation of the phagocytosis of B16 cells by macrophages (MØ). B16 cells were transfected by 3 mg/mL of STAVs for 3 hr and irradiated by UV (120 mJ/cm²). The irradiated B16 cells were fed to macrophages (MØ) at 24 hr after UV irradiation. (B) Confocal microscopy analysis of macrophages following cellular engulfment of B16 cells transfected with FAM-labeled STAV. (C) qRT-PCR analysis of Cxcl10 in WT and STING knock out macrophages (WT MØ and SKO MØ) following engulfment of B16 cells in presence or absence of STAVs.

STAVs are an effective cell-based therapy for breast cancer

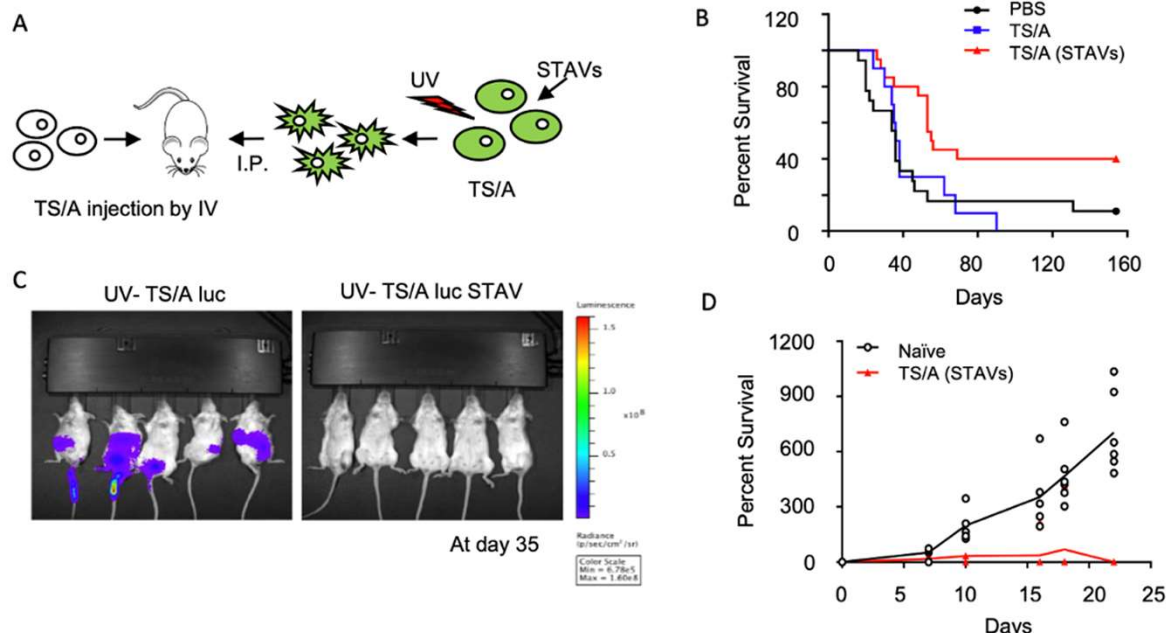
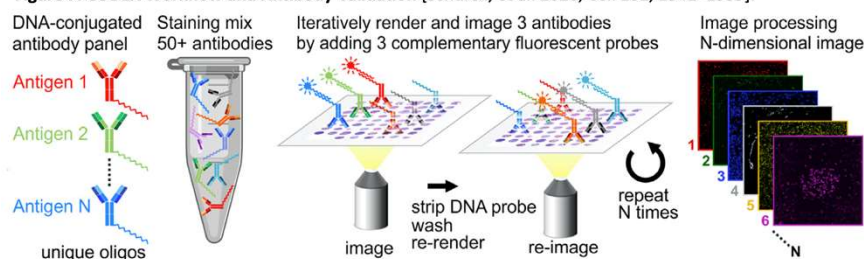


Figure 4. Effect of UV-irradiated, STAV-treated TS/A breast carcinoma cells in IV TS/A lung metastasis model. (A) Schematic representation of experimental design; (B) TS/A (STAVs)-treated, UV-irradiated cells prolong survival ($N=20/\text{group}$, $p=0.008$); (C) Day 35 luciferase activity in UV-TS/A (luc) STAV-treated (right) mice as compared control-treated mice (left); (D) TS/A-luc STAV-treated mice rechallenged with TS/A-luc Cells (1×10^5) vs. naïve mice controls (6/group; $p=0.03$).

Figure 7. CODEX Workflow and Antibody Validation [Schurch, et al. 2020, Cell 182, 1341–1359].



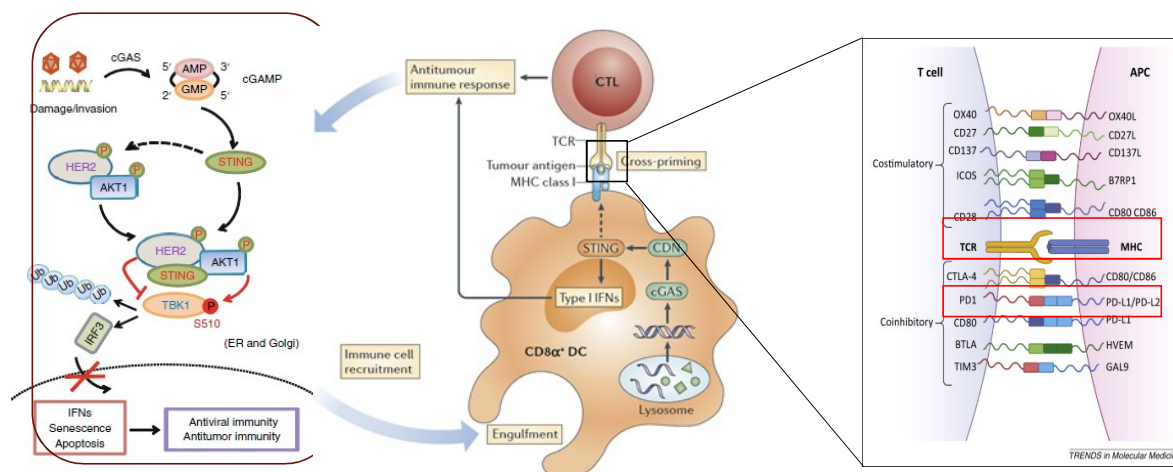
We hypothesize that UV-irradiated, STAV-transduced, autologous breast tumor cells may provide effective cell-based immunotherapy for the treatment of breast cancer.

Aim 1 – Elucidate the mechanism(s) responsible for attenuation of cGAS-STING signaling by constitutive HER2 kinase activation resulting from gene amplification/overexpression.

Aim 2 -- To confirm the efficacy and safety of parenteral administration of UV-irradiated, STAV-transduced syngeneic breast carcinoma cells in a syngeneic immunocompetent orthotopic (4T1-luc, BALB/c) mouse model of breast cancer, and human orthotopic PDXs in immune cell reconstituted (Hu-NSG-SGM3) mice, and to characterize the anti-tumor immune response using multiplexed DNA-tagged antibody staining (co-detection by indexing, CODEX -- technology pioneered at the Stanford Cell Sciences Imaging Facility).

Aim 3 – Determine whether STAV-induced adaptive immune responses resulting in breast tumor growth inhibition in vivo can be further augmented by immune checkpoint inhibition with anti-PD-1 antibody.

Reconstituting cGAS-STING signaling in HER2+ breast cancer: Summary



1. The detection of pathogens through nucleic acid sensors is a defining principle of innate immunity. DNA-sensing receptors sample subcellular compartments for foreign nucleic acids and, upon recognition, trigger immune signaling pathways for host defense.
2. Aberrant DNA fragments are ubiquitous in cancer cells due to abnormal chromosome structure, genome instability and post-radiation/chemo effects, which can be sensed by cGAS–STING. It is hypothesized evading damage surveillance is therefore necessary in tumorigenesis and tumor progression.
3. HER2 kinase inhibits cGAS–STING signaling, and prevents breast cancer cells from producing cytokines; cGAS-STING signaling may be reconstituted by anti-HER2 treatment.
4. Defects in STING signaling may enable HER2+ cells to escape cytokine production triggered by catastrophic DNA damaging events which would otherwise facilitate their eradication via the immune-surveillance system.

A corollary to this hypothesis is that pharmacologic STING activation in concert with HER2 blockade will reconstitute the cGAS-STING innate immune signaling, setting the stage for therapeutic strategies aimed at amplifying effective adaptive anti-tumor responses.

Questions/Comments Criticism/Debate



Glen Barber
Hiroki Ishikawa
Jeonghyun Ahn



- Amy Zong
- Xiaofei Lin
- Wen Liang

THANK YOU!

Stanford Cell Sciences Imaging Facility

